A one dimensional model of Earth structure in the western United States from GPS observations of ocean tidal load

Takeo Ito #1,#2 and Mark Simons #2
#1Nagoya University, Japan #2 Caltech

1.Abstract

We generate 702 high-rate (5 min samples) 3-component GPS time series for the western United States for the year 2008 using a kinematic positioning strategy. We decompose the resulting time series into solid Earth body tides and the ocean tidal loading (OTL) components. From the GPS time series, we estimate east, north, and vertical OTL response for 5 major tidal constituents (M2, S2, O1, N2 and Q1). We used these measurements to construct a 1D model of the elastic and density structure of the western United States.

The observed OTL response at each GPS site is the result of convolving the spatially and temporally variable OTL with the regional elastic response of the earth. The measurement of the OTL displacement with GPS has seen much progress in recent years [King et al., 2008, Thomas et al., 2007] demonstrating an attainable measurement quality of better than 1 mm. Ideally, the OTL displacement should be predicatable at least to this accuracy. The OTL can be well-predicted by global ocean tideal models derived from assimilation of satellite altimetry and tide-gauge data.

We use our estimates of the OTL response to construct images of material property variations in the shallow mantle. Unlike seismic data, OTL responses depend directly on the elastic properties as opposed to indirectly through the seismic velocity. Thus, in the future, these OTL-based elastic models will provide useful comparison with seismically derived models - noting of course, that our observations are made at much longer periods than typical seismic observations.

2.GPS array and OTL model setting

We applied kinematic GPS analysis with the GpsTools (GT) ver.0.6.4 software [Takasu and Kasai, 2005] to estimate the position of 702 GPS sites every 5 min for the year 2008. Fig.1 shows the time series of displacemnets at site P224, located near San Francisco Bay (see Fig.1). The positions are estimated without tidal corrections. Sub-daily time series of displacements at GPS are affected by solid Earth body tides and OTL displacement. The OTL can be predicted using a global ocean tide model (for example FES2004, see Fig.1), derived from assimilation of satellite altimetry and tide-gauge data. From each GPS time series, we remove the effects of solid Earth body tides using a model, in principle leaving the effects of OTL (see Fig. 2).

Observation = Solid Body tide + OTL disp. + err.

Effect of solid Earth body tides

Theoretical solid Earth body tide components are well known. The contributions from the tides are expressed in terms of Love numbers. In our correction for solid body tides, we uses complex Love numbers to spherical harmonic degree 3 for 500 tidal constituents. These values and corrections methods follow IERS Convention (2003) and the HW95 tidal potential catalogue [Hartmann and Wenzel, 1995].

OTL displacement

For all 3 components of each GPS site, we estimate the OTL displacement for 15 constitutes: M2, K1, S2, O1, P1, N2, K2, Mf, Q1, Mm, 2N2, Mtm, S1, M4 and Msqm. The time series of differences between the observation and the solid Earth body tide is expressed as:

$$O(t) = \sum_{i=1}^{15}\left(A_i\cos(\varphi_i t) + B_i\sin(\varphi_i t)\right) + \sum_{n=3}^{\infty}\left(C_n\cos(n\varphi_{sidereal}\, t) + D_n\sin(n\varphi_{sidereal}\, t)\right) + e(t)$$

where φ_i is the angular velocity of i th constituent and $\varphi_{sidereal}$ is the angular velocity (15.04106864 degree/hour) of the sidereal day.

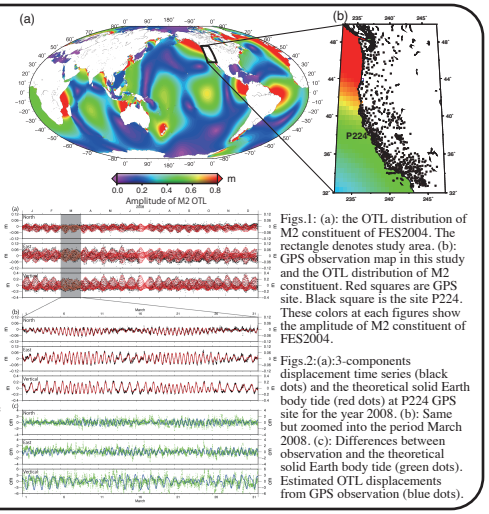

Figs.1: (a): the OTL distribution of M2 constituent of FES2004. The rectangle denotes study area. (b): GPS observation map in this study and the OTL distribution of M2 constituent. Red squares are GPS site. Black square is the site P224. These colors at each figures show the amplitude of M2 constituent of FES2004.

Figs.2:(a):3-components displacement time series (black dots) and the theoretical solid Earth body tide (red dots) at P224 GPS site for the year 2008. (b): Same but zoomed into the period March 2008. (c): Differences between observation and the theoretical solid Earth body tide (green dots). Estimated OTL displacements from GPS observation (blue dots).

3. Green function and Sensitivity Kernel

To compute the OTL displacement, we use a convolution of the tidal ocean height with a point load response Green' s function. We describe the OTL using 205,354 point loads of variable dimension. For our Green' s function, we adopt the spherically symmetrical, non-rotating, perfectly elastic and isotropic (SNREI) Earth model. We use assymptotic expressions to compute the Legendre series in the Green' s functions for the load Love numbers [Farrell, 1972]. We employ a method which is one order of magnitude more accurate than Farrell' s solution [Guo et al., 2004].

In order to estimate subsurface elastic structure, we calculate the sensitivity kernel of the Green' s function. We define the Greens function as $G(R,\mathbf{S})$. Here, R and $\mathbf{S}$ are distance and structure, respectively. We can write the sensitivity kernel as follow:

$$Sk(R,\mathbf{S}) = \frac{G(R,\mathbf{S}+\delta\mathbf{S})}{G(R,\mathbf{S})}$$

where, $\delta\mathbf{S}$ is perturbation. Fig. 4 shows the sensitivity of Green' s function.

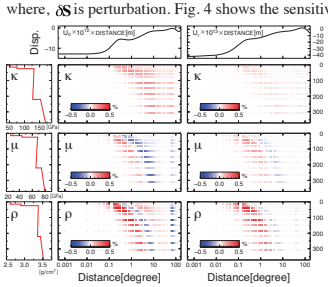

Fig. 4: Sensitivity and absolute value for Green' s functions, and structure. Left and middle figures relate to horizontal and vertical components, respectively. Right figures are structure models for each components. Top figures denote the absolute value (normalized as in Farrell (1972)) of Green' s functions for each components (horizontal and vertical). The 2nd, 3rd and 4th rows are sensitivity kernel map of each component, respectively. Red and blue colors show positive and negative sensitivity of Greens function.

Note: That in the top panels, The predicted disp are multiplied by the distance from the load.

4. Spatial distribution of OTL response

We can now map out the spatial distribution of the OTL response field for each tidal constituent. This spatial pattern of the OTL response is largely controlled by the OTL distribution. For all constituents, the vertical is the largest component. The standard deviation of the residuals after removing the best fit OTL response coefficients for each tidal constituent and component show no systematic geographic patterns, suggesting that we have a reasonable estimate of the OTL response (see Figs 5).

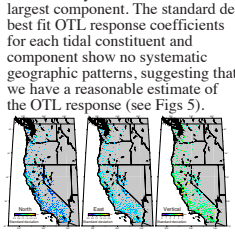

Figs 5: Spatial variation of standard deviation of GPS observation for the 3-components.

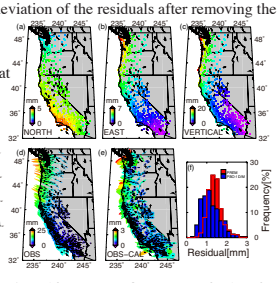

Figs 6: (a)-(c): Spatial distribution of the estimated 3-component OTL response for the M2 tidal constituent. (d): Elliptical plot of spatial distribution of the observed OTL response for the M2 tidal constituent. Major and minor axes of ellipse are maximum and minimum amplitude including 3-components, respectively. Color means maximum amplitude. (e): Elliptical plot of spatial distribution of the observed OTL response against the predicted OTL response at M2 tidal constitutes using PBO-1D/M. Detail of same as (d). (f): Histograms of residual of the observed OTL response against the predicted OTL response at M2 tidal constituent. Red bins: The predicted OTL response based on FES2004 and PREM. Bule bins: Based on PBO-1D/M.

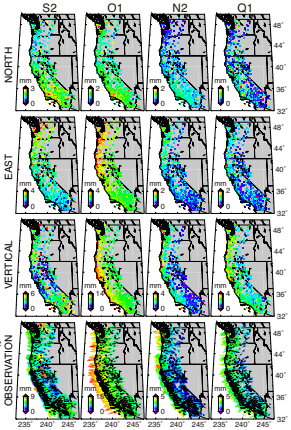

Figs 7: Spatial distribution of the observed 3-component OTL response for the S1, O1, N2 and Q1 tidal constituents. Top, second and third columns are north, east and vertical component of OTL response, respectively. Fourth row is elliptical plot of spatial distribution of the observed OTL response. Detail of description is same as figure 6 (d).

5. Inversion method and Result

We use 10,530 amplitudes and phases of the observed OTL displacements. Our 1-D model of $\varkappa$, μ, and ϱ is parameterized with 13 layers at depths shallower than 355 km and includes ability to have discrete discontinuities at depths of 15, 24.4 and 220 km. Let $\mathbf{d}$ be an observed OTL displacement vecter and let $\mathbf{m}$ denote an unknown model parameter consisting of the two elastic moduli $\varkappa$, μ, and the mass density ϱ. We pose the problem in terms of logarithms of each quantity:

$$\mathbf{m}=\{\log\frac{\varkappa}{\varkappa_0}, \log\frac{\mu}{\mu_0}, \log\frac{\varrho}{\varrho_0}\}$$

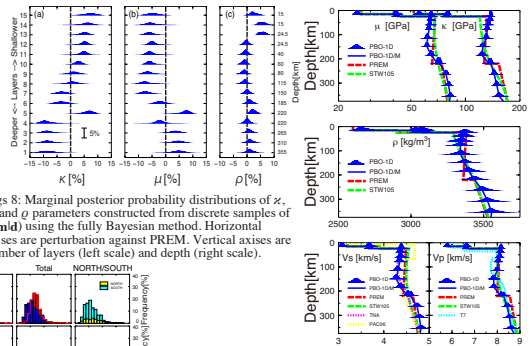

Figs 8: Marginal posterior probability distributions of $\varkappa$, μ, and ϱ parameters constructed from discrete samples of $\mathbf{p}(\mathbf{m}|\mathbf{d})$ using the fully Bayesian method. Horizontal axises are perturbation against PREM. Vertical axises are number of layers (left scale) and depth (right scale).

In order to estimate a 1-D model, we solve a non-linear observation equation:

$$\mathbf{d} = \mathbf{g}(\mathrm{m}) + \varepsilon.$$

where $\mathbf{g}$(m) gives the theoretical relationship between the vector of OTL response, $\mathbf{d}$, and the vector of subsurface structure, $\mathbf{m}$. We adopt a fully probabilistic approach, where the posterior PDFs result from a product of a likelihood based on data misfit. The complete solution to the inverse problem, the posterior probability density function of elastic moduli and density structure, is formulated using Bayes theorem and sampled with a Markov Chain Monte Carlo method (MCMC).

Using PREM as our initial model, we obtain posterior PDFs of a new radial model that is consistent with our set of OTL response data. We call this model PBO-1D (see Figs 9). PBO-1D/M means median of PBO-1D. Based on our sensitivity analysis and exploring the role of using different models, we conclude that PBO-1D only has sensitivity in the upper 350 km of the mantle.

Relative to PREM, the primary features of PBO-1D include a region of higher elastic moduli in the crust, lower elastic moduli at depths between 100 and 200 km and a strong preference for models that do not include a discontinuity at 220 km depth. In order to evaluate resolution and confidence of unknown parameters, we calculate covariance (see Figs 12). It actually has tiny correlation between each component. These correlation between each component are less than 0.3 and positive. This positive correlation means that ratio of each component is constant. Hence, variances of P and S wave velocities are better than other properties.

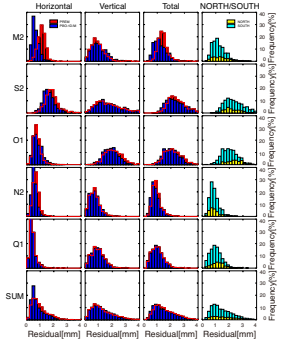

Figs 11: Histograms of residual of the observed OTL response versus the predicted OTL response by PBO-1D/M. Row left to right are north, east, vertical components, and north and south in the residual composition, respectively. Column top to bottom are M2, S2, O1, N2, Q1, and the sum of all sum up five tidal constitutes. Red bins: The predicted OTL response based on FES2004 and PREM. Bule bins: Based on PBO-1D/M. Yellow bins: Associate with North region (latitudes above 40 N). Light blue bins: Associate with North region (latitudes below 40 N).

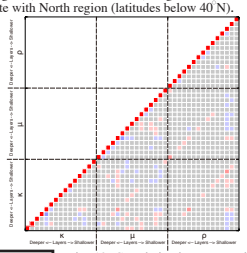

Figs 12: Correlation between each posterior probability distributions **m**.

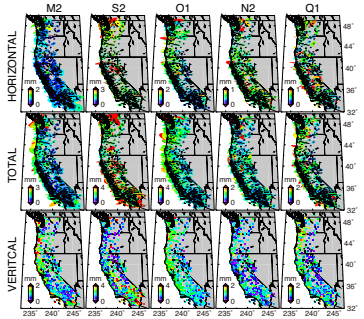

Figs 10: Spatial distribution of residual of the observed OTL response against the predicted OLT response by PBO-1D/M.

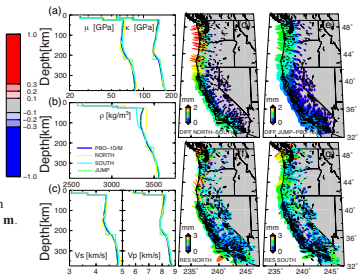

Figs 13: (a)-(c): Comparison of 1-D models. NORTH: Estimated using only GPS sites latitudes above 40 N. SOUTH: Using only GPS sites latitudes below 40 N. JUMP: Artificially constructed to be the same as PBO-1D/M but with a PREM-like jump at 220 km depth. (d)-(g): Elliptical plot of the spatial distribution of the M2 tidal constituent. (d): The differential OTL response between NORTH and SOUTH models in (a)-(c). (e): The differential OTL response between JUMP and PBO-1D/M models in (a)-(c). (f)-(g): Spatial distribution of the residual of the observed OTL response against the predicted OTL response from NORTH (f) and SOUTH (g) models.

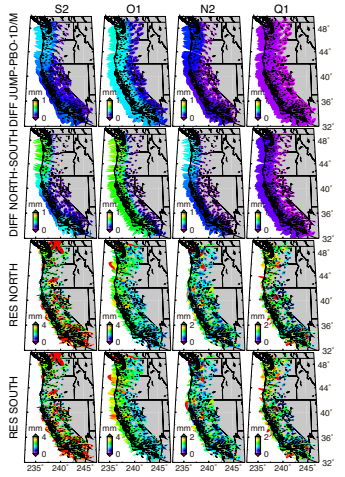

Figs 14: Top: Differences between JUMP and PBO-1D/M models. Second column: Differences between NORTH and SOUTH models. Third column: Residual of north model. Bottom: Residual of south model. Row left to right are M2, S2, O1, N2, and Q1, respectively. These figure are considering 3-components.